Journal of Applied Polymer Science

Preparation of Polymer Electrolytes Based on the Polymerized Imidazolium Ionic Liquid and Their Applications in Lithium Batteries

Mingtao Li, Lu Wang, Tingting Du
Department of Chemical Engineering, School of Chemical Engineering and Technology, Xi'an Jiaotong University, Xi'an Shaanxi 710049, China
Correspondence to: M. Li (E-mail: lmt01558@mail.xjtu.edu.cn)

ABSTRACT: The polymer electrolytes based on a polymerized ionic liquid (PIL) as polymer host and containing 1,2-dimethyl-3-butylimidazolium bis(trifluoromethanesulfonyl)imide (BMMIM-TFSI) ionic liquid, lithium TFSI salt, and nanosilica are prepared. The PIL electrolyte presents a high ionic conductivity, and it is 1.07×10^{-3} S cm^{-1} at 60°C, when the BMMIM-TFSI content reaches 60% (the weight ratio of BMMIM-TFSI/PIL). Furthermore, the electrolyte exhibits wide electrochemical stability window and good lithium stripping/plating performance. Preliminary battery tests show that Li/$LiFePO_4$ cells with the PIL electrolytes are capable to deliver above 146 mAh g^{-1} at 60°C with very good capacity retention. © 2014 Wiley Periodicals, Inc. J. Appl. Polym. Sci. **2014**, *131*, 40928.

KEYWORDS: batteries and fuel cells; electrochemistry; polyelectrolytes

Received 23 February 2014; accepted 27 April 2014
DOI: 10.1002/app.40928

INTRODUCTION

Recently, polymerized ionic liquids (PILs) have attracted much interest because of their potentially wide-range applications including uses in catalysis,[1] gas separation membranes,[2] porous polymer materials,[3] nanomaterial synthesis,[4] and polymer electrolytes for lithium batteries[5] and dye-sensitized solar cells.[6] Particularly, PILs as solid polymer electrolytes receive significant attention in the field of lithium batteries because they may avoid some disadvantages of liquid electrolytes, such as leakage and flammability. In addition, the polymer nature of PIL electrolytes potentially permits production of batteries with defined size, shape, and geometry, such as thin film forms. Although the PIL electrolytes alleviate the shortcomings of liquid electrolytes, they usually possess lower ionic conductivity when compared with the latter. Therefore, recently, a number of investigations focus on the enhancement of ionic conductivity and exploring the factors that may impact ionic conductivity in PILs, such as polymer chemistry, glass transition temperature, molecular weight, and polymer morphology.

One method for increasing the ionic conductivity in a PIL electrolyte is to introduce flexible pendant groups in cation structure of PILs. For example, Lee et al.[7] reported a series of PILs based on imidazolium cations containing flexible ethylene oxide pendant groups. They found that as the length of the ethylene oxide pendant group in the PILs increased, the glass transition temperature of PIL decreased and the ionic conductivity increased, implying that the introduction of ethylene oxide pendant group on the imidazolium cation improved the chain mobility of the resulting PIL. The ionic conductivity of the PIL electrolyte reached 3×10^{-5} S cm^{-1} at room temperature. The second method for increasing the ionic conductivity in a PIL is to replace the mobile anion with another via anion exchange. Chen et al.[8] found enhancements in ionic conductivity in a PIL when the tetrafluoroborate (BF_4) anion was replaced by the bis(trifluoromethanesulfonyl)imide (TFSI) anion. This was the result of a significant decrease in the glass transition temperature of the polymer, which facilitated higher segmental motion of the polymer and hence higher anion mobility. Although the enhanced ionic conductivity has been obtained, these solid PIL electrolytes still cannot meet the requirement of lithium batteries. Generally, lithium batteries demand solid polymer electrolyte membranes having ionic conductivity more than 10^{-4} S cm^{-1} at room temperature.[9] In addition to the lower ionic conductivity, the high interfacial impedance between electrode and solid PIL electrolyte presents a far more severe problem to the ion transport than the bulk ion conduction does.[10]

Recently, the incorporation of ionic liquid into PIL matrices has been used to prepare PIL + ionic liquid gel membranes.[11,12] The gel electrolytes possess higher ionic conductivity as well as good electrode–electrolyte contact and therefore reduced interfacial impedance when compared with solid PIL electrolyte, which makes them more suitable for solid-state lithium battery applications. In several previous studies, we have prepared a series of gel electrolytes based on various copolymer-type PILs and incorporating IL, lithium salt, and nanosilica, and their performances in lithium batteries have been evaluated at a high

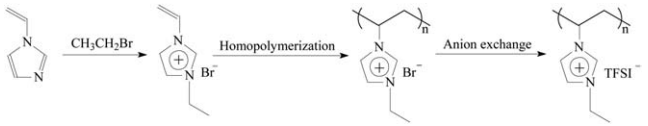

Scheme 1. Illustration for the synthesis of the PILs.

temperature (80°C).[13–15] However, at a decreased temperature, the battery performances are not favorable. The reason may be the copolymer composition in these electrolyte systems cannot provide ion conduction, and even hinder the ion transport, resulting in relatively low ionic conductivity and thus unfavorable battery performances. Therefore, a homo-PIL polymerized only by IL monomer may benefit the ion conduction.

In this study, a new kind of homo-PIL based on imidazolium cations was synthesized by free radical polymerization and an ion exchange reaction (see Scheme 1). Then, gel PIL electrolyte membranes were prepared by incorporating an imidazolium-based IL, lithium salt and nanosilica in the PIL host. Nanosilica added in the electrolytes was to decrease the adhesion of the PIL membranes and thus the membranes can be handled easily. The PIL electrolyte was used in Li/$LiFePO_4$ cells and showed good performances at current rates of 0.1 C and 60°C.

EXPERIMENTAL

Reagents and Materials

1-Vinylimidazole and *n*-butylbromide were purchased from Alfa Aesar. Lithium TFSI (LiTFSI) was kindly provided by Morita Chemical Industries and used as received. Nanosilica (fine reagent grade) with average diameter of 30 nm was purchased from Aladdin. All the other chemicals used in this work were of analytical grade reagent.

Synthesis of the Monomer

1-Vinylimidazole was treated with 1.2 equiv of ethylbromide in tetrahydrofuran and stirred for 48 h. The solution was washed with large amounts of diethyl ether. The precipitate obtained was filtered and recrystallized in tetrahydrofuran–ethanol solvent. The structure was confirmed by ^{1}H-NMR.

1-Vinyl-3-ethylimidazolium bromide (VE-Br): ^{1}H-NMR (400 MHz, $CDCl_3$), δ (TMS, ppm): 7.83 (NC*H*N), 7.67 (CHNC*H*CHNCH$_2$), 7.48 (CHNCHC*H*NCH$_2$), 7.42 (NC*H*CH$_2$), 6.03 (NCHC*H*$_2$), 5.40 (NCHC*H*$_2$), 4.48 (NC*H*$_2$CH$_3$), 1.65 (NCH$_2$C*H*$_3$).

Synthesis of the PIL with TFSI Anions

The synthesis route of the PIL with TFSI anions is illustrated in Scheme 1. VE-Br (2.0 g), dimethylsulfoxide (12 mL) and 2,2′-azobis(2-methylpropionitrile) (0.004 g) were mixed until they became homogeneous. The mixture was degassed in vacuum at 40°C and kept constant at 70°C for 12 h. After polymerization, the mixture solution was rinsed three times with large amounts of acetone, and the solid polymer 1.72 g (86% yield) was obtained, denoted as PVE-Br. Then, the PVE-Br was dried at 60°C for 12 h. After a simple ion-exchange reaction, the PIL with TFSI anions was obtained as follows: 4.5 g of PVE-Br was dissolved in 5 mL deionized water, stirred for 2 h, and then lithium salts (LiTFSI) of which amount is 6.8 g was added into the solution and was stirred for another 4 h. After the ion-exchange reaction finished, the solid product was put into the Teflon dishes, immersed in deionized water at 40°C for 1 h, and rinsed with large amounts of deionized water. The process of immersion and rinse was repeated twice so as to remove the superfluous lithium salts. Then, the polymer denoted as PVE-TFSI was dried in vacuum at 90°C for 24 h, and the pure product was obtained.

Structures of the PVE-Br and the PVE-TFSI (depicted in Scheme 1) were confirmed by ^{1}H-NMR and FTIR.

PVE-Br: ^{1}H-NMR (400 MHz, CD_3OD), δ (TMS, ppm): 8.22–7.52 (C*H*NC*H*C*H*N), 4.82 (CH$_2$C*H*N), 3.11 (NC*H*$_2$CH$_3$), 2.64 (C*H*$_2$CHN), 1.60 (NCH$_2$C*H*$_3$). PVE-Br: FTIR (KBr), ν (cm^{-1}): 3434 (H$_2$O), 3140, 3062, 2985, 2932, 2854 (CH, CH$_2$, CH$_3$), 1642 (C═C), 1557 (C═N), 1434 (C—N). M_n = 14,250, M_w/M_n = 2.76 (GPC, polystyrene).

PVE-TFSI: FTIR (KBr), ν (cm^{-1}): 3408 (H$_2$O), 3134, 3076, 2990, 2926, 2847 (CH, CH$_2$, CH$_3$), 1636 (C═C), 1558 (C═N), 1434 (C—N), (TFSI$^-$): 1212, 1173, 1056, 788, and 730.

Preparation of the IL (BMMIM-TFSI)

The IL 1,2-dimethyl-3-butyl-imidazolium TFSI (BMMIM-TFSI) was synthesized according to the methods proposed in Refs. 16 and [17]. 1,2-Dimethyl-imidazole was treated with 1.2 equiv of *n*-butylbromide in ethanol and stirred for 48 h. The solution was washed with large amounts of diethyl ether. The precipitate was filtered and recrystallized in tetrahydrofuran–ethanol solvent. Then, the pure 1,2-dimethyl-3-butylimidazolium bromide was obtained. Recrystallized 1,2-dimethyl-3-butyl-imidazolium bromide was treated with exactly 1.0 equiv of LiTFSI in water for 5 h. After the reaction, the mixture was separated into two phases, with the bottom phase being BMMIM-TFSI. The ionic liquid was extracted twice with chloroform, and combined organic solution was washed twice with deionized water. It was then concentrated by rotary evaporation in vacuum. After dried in vacuum at 110°C for 12 h, the pure BMMIM-TFSI (see Scheme 2) was obtained. The structure was confirmed by ^{1}H-NMR spectra.

BMMIM-TFSI: ^{1}H-NMR (400 MHz, acetone-d_6), δ (TMS, ppm): 7.64 (d, 1H), 7.56 (d, 1H), 4.15 (t, 2H), 3.92 (s, 3H), 3.77 (s, 3H), 1.97 (m, 2H), 1.39 (m, 2H), 0.96 (t, 3H).

Preparation of the Polymer Gel Electrolytes

The polymer gel electrolytes were prepared by separately dissolving the PVE-TFSI, BMMIM-TFSI, LiTFSI, and nanoscale SiO_2 in acetone at 40°C for 5 h and then mixed in three different proportions (see Table I). The solution was casted onto PTFE slides to prepare the electrolyte films. Then, the film was dried in the nitrogen atmosphere at room temperature for 12 h and subsequently dried at 80°C under vacuum for another 12 h.

Preparation of Batteries

Lithium foil (battery grade) was used as a negative electrode. The positive electrode was fabricated by spreading the mixture of $LiFePO_4$, acetylene black, and PVDF (initially dissolved in *N*-

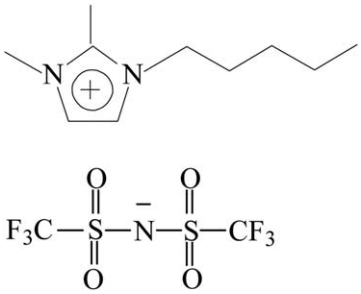

Scheme 2. Molecular structure of the IL (BMMIM-TFSI).

methyl-2-pyrrolidone) with a weight ratio of 8 : 1 : 1 onto Al current collector (battery use). Loading of active material was about 2.5 mg cm^{-2} corresponding to 0.4 mAh cm^{-2}, and this thinner electrode was directly used without pressing. Li/$LiFePO_4$ polymer batteries were fabricated (in an argon-filled glove box) by laminating the lithium foil, with a PIL-IL-LiTFSI-SiO_2 polymer electrolyte membrane and a $LiFePO_4$ cathode tape.

Characterization Methods

Structures of the synthesized ionic liquid and the PILs were confirmed by ^{1}H-NMR spectroscopy (Avance III 400), and tetramethylsilane was used as the internal reference for the analysis. The FTIR spectroscopic measurements were performed on a Bruker IFS-28 FTIR spectrometer. Thermal analyses of the polymers were performed on a Perkin-Elmer thermogravimetric analyzer from room temperature to 400°C under nitrogen at a heating rate of 20°C min^{-1}. Molecular weights of the polymers were determined on Waters 717 Plus autosampler gel permeation chromatography apparatus equipped with Waters RH columns and a Dawn Eos (Wyatt Technology) multiangle laser light scattering detector using 12 monodisperse polystyrenes (molecular weight range of 10^2-10^7) as calibration standards. The sample solutions were prepared in *N*,*N*-dimethylformamide (ca. 2 mg mL^{-1}) and filtered through 0.45-μm poly(tetrafluoroethylene) syringe-type filters before injected into the GPC system.

The ionic conductivity of the PILs was measured by the complex impedance method using a CHI660D Electrochemical Workstation. The electrolytes were placed between a pair of blocking electrodes. The data were collected over a frequency range of 0.1–10^5 Hz with the amplitude of 5 mV for an open-circuit potential. The ionic conductivity (σ) was calculated from the bulk electrolyte resistance value (R) found in the complex impedance diagram according to the following equation:

$$\sigma = L/R \times S,$$

where L is the thickness of the polymer electrolyte film, and S is the area of the polymer electrolyte film.

The electrochemical stability of the PILs electrolytes was determined on the CHI660D Electrochemical Workstation by linear sweep voltammetry (LSV) using the cell Li/PILs electrolyte/stainless steel (SS), in which SS was used as the working electrode, lithium as the reference, and the counter electrodes. The scanning rate is 10 mV s^{-1}.

Preliminary cycling tests on Li/$LiFePO_4$ polymer batteries were performed at 60°C using a CT2001A cell test instrument (LAND Electronic). The charge and discharge current rates were fixed to C/10. The voltage cutoffs were fixed at 4.0 (charge step) and 2.0 V (discharge step).

RESULTS AND DISCUSSION

Characterization of PILs

Structures of the monomer VE-Br and the PIL PVE-Br were confirmed by ^{1}H-NMR spectra, as shown in Figure 1(a,b). For the monomer VE-Br, the characteristic proton absorptions in double bonds locate at δ (ppm) = 7.42 (NC*H*CH_2), 6.03 (NCHCH_2), and 5.40 (NCHCH_2), and after polymerization, the absorptions completely disappear in the PVB-Cl structure, as shown in Figure 1(b), indicating that the polymerization carries out entirely and the product is relatively pure. Simultaneously, the new proton absorptions appear, such as δ (ppm) = 4.82 (CH_2CHN) and 2.64 (CH_2CHN). In addition, the proton absorptions of δ (ppm) = 7.83 (NC*H*N), 7.67 (CHNC*H* CHNCH_2), and 7.48 (CHNCHC*H*NCH_2) in Figure 1(a) resulting from the characteristic absorptions of imidazolium cations still exist in the spectra of PVE-Br after the polymerization. All the assignments of protons have been marked in Figure 1.

Figure 2 shows the FTIR spectra of the obtained PILs having $TFSI^-$ counter anions after anion exchange reaction and the initial PILs having Br^- anions. When compared with the spectra of PVE-TFSI with PVE-Br, it is obvious that some new bands appear attributed to the new different anions $TFSI^-$, which are located at 1212, 1173, 1056, 788, and 730 cm^{-1}.[18,19] Furthermore, the characteristic bands at 1642 and 1557 cm^{-1} for the C═C and C═N stretching vibration, respectively, arise from the imidazolium ring, and the characteristic band at 1434 cm^{-1} arises from C—N stretching vibration in the FTIR spectra of PVB-TFSI, indicating that the structure of the polymer backbone is maintained after the anion exchange reaction. In addition, broad peaks near 3434 cm^{-1} in the FTIR spectra are from

Table I. Composition of PIL-(BMMIM-TFSI)-LiTFSI-SiO_2 Gel Polymer Electrolytes

Sample name	Weight (g)				BMMIM-TFSI/PIL ratio (wt/wt)
	PIL	LiTFSI	Nanoscale SiO_2	BMMIM-TFSI	
PVE-IL-0.40	0.8	0.16	0.08	0.32	0.40
PVE-IL-0.45	0.8	0.16	0.08	0.36	0.45
PVE-IL-0.50	0.8	0.16	0.08	0.40	0.50

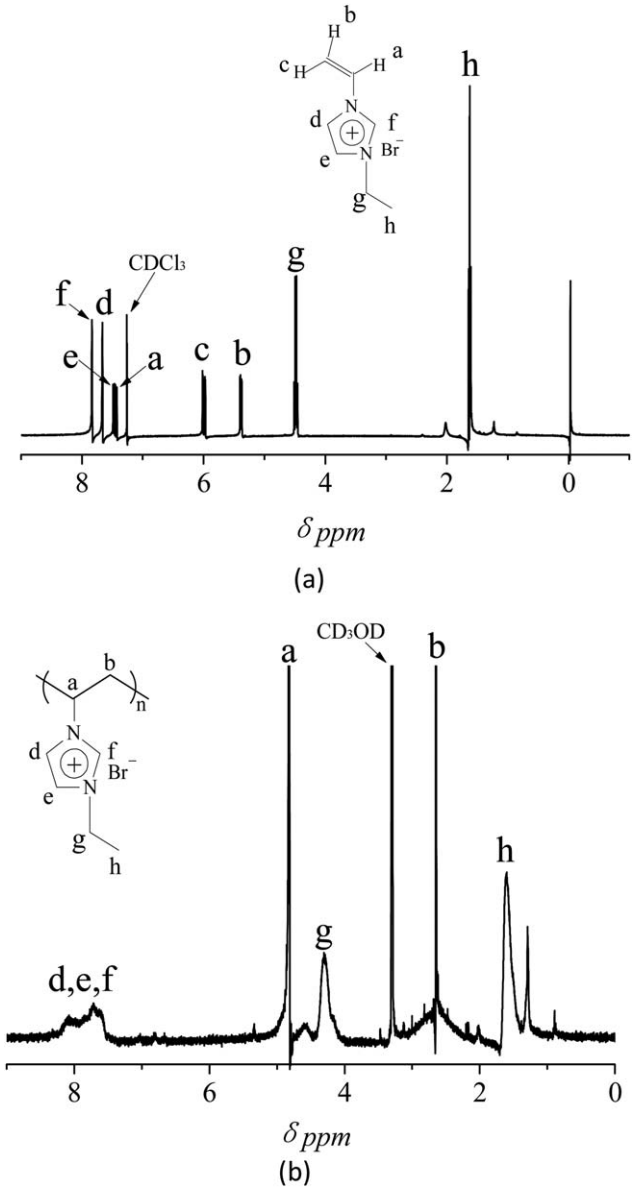

Figure 1. [1]H-NMR spectra of (a) VE-Br and (b) PVE-Br.

moisture. We have repeated several FTIR tests, but the peaks still exist. Although the PIL samples are dried well before tests, they absorb humidity when exposed to air. To avoid the samples from absorbing moisture, the following electrochemical tests were all performed in an argon-filled UNLAB glove box ($[O_2] < 1$ ppm; $[H_2O] < 1$ ppm). According to the analysis, it is concluded that the FTIR spectra constitute an indication of the anion exchange.

Gel Polymer Electrolytes Based on the PIL

At the aim of application in lithium batteries, a gel polymer electrolyte membrane based on PVE-TFSI as the polymer host was prepared, incorporating BMMIM-TFSI ionic liquid, LiTFSI salt, and nanosize SiO_2. The addition of ILs into polymer electrolytes could improve the interfacial property toward the electrode material and increase the lithium ionic conductivity.[11,20]

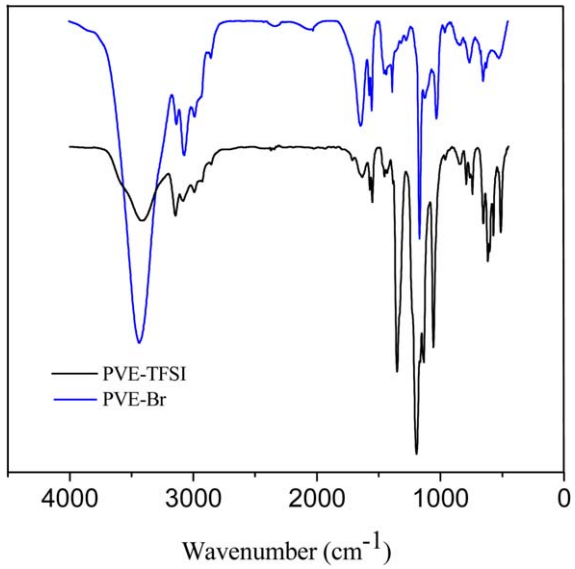

Figure 2. FTIR spectra of PVE-Br and PVE-TFSI. [Color figure can be viewed in the online issue, which is available at wileyonlinelibrary.com.]

BMMIM-TFSI was used here because of its good electrochemical properties and exceptional battery performance as electrolyte.[21,22] Nanosize SiO_2 was also added in this gel polymer electrolyte as it could decrease the adhesion of the PIL membrane, which indicates that the membrane can be handled easily.[23–26]

Thermal Stability

The thermal stability of the pure PIL and PIL-based electrolytes was characterized by thermogravimetric analysis, as shown in Figure 3. It is obvious that the thermal stabilities of the PIL-based electrolytes are affected by the BMMIM-TFSI content. Their decomposition temperatures increase markedly with the IL content, which is due to the high decomposition temperatures of BMMIM-TFSI.[27] The PIL-based electrolyte

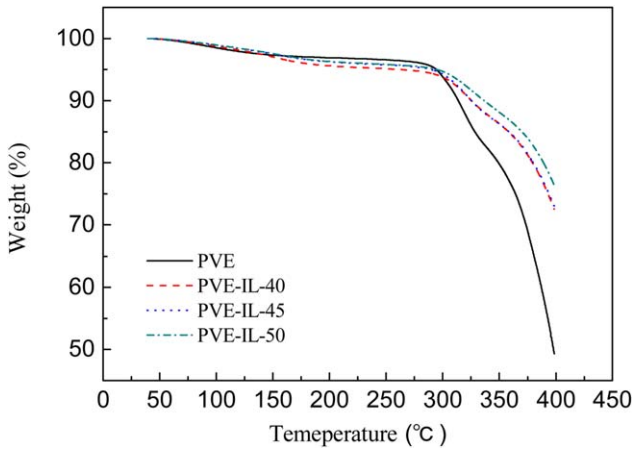

Figure 3. Thermogravimetric analysis profiles of pure PIL, PVE-TFSI, and PIL-(BMMIM-TFSI)-LiTFSI-SiO_2 polymer electrolytes with different BMMIM-TFSI amounts. [Color figure can be viewed in the online issue, which is available at wileyonlinelibrary.com.]

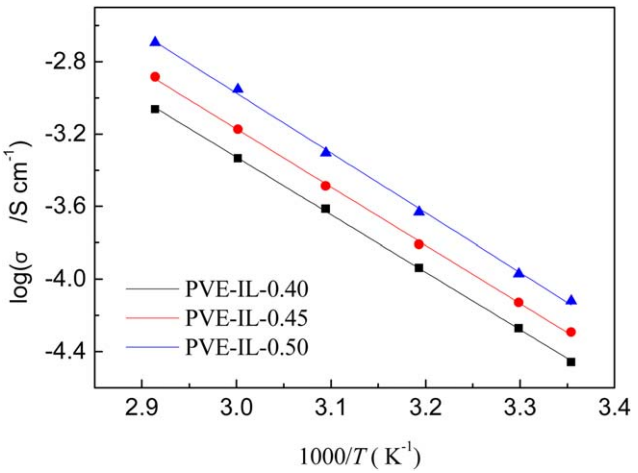

Figure 4. Temperature dependence of the ionic conductivity of PIL-(BMMIM-TFSI)-LiTFSI-SiO_2 electrolyte samples with different BMMIM-TFSI amounts. [Color figure can be viewed in the online issue, which is available at wileyonlinelibrary.com.]

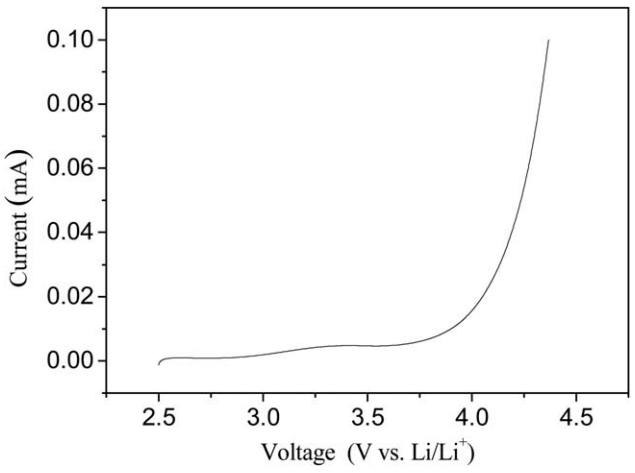

Figure 5. Electrochemical stability of PVE-IL-0.50 electrolyte samples (Li/PIL electrolyte/SS cell, 10 mV s^{-1}, 2.5–4.5 V; SS, stainless steel).

samples are found to be thermally stable at temperature more than 320°C.

Ionic Conductivity

Figure 4 shows the temperature dependence of the ionic conductivity of PIL-based electrolyte samples, and the corresponding values of the ionic conductivity are listed in Table II. For the samples, linear increases were observed in the conductivity values with temperature, which fitted an Arrehenius equation:

$$\sigma(T) = A \times \exp\left(\frac{-E_a}{RT}\right),$$

where A is the pre-exponential factor, E_a is the activation energy for ionic conductivity, and T is the absolute temperature value, typically obtained in completely amorphous phase ionic conductivity.[28] In polymer electrolyte systems, the change of conductivity with temperature may be due to the segmental motion of the polymer chains leading to increase in free volume in the system, which will provide an easy pathway for the transitional motion of the ions. The segmental motion also permits the ions to hop from one site to another. As the temperature increases, both the segmental motion and transitional ionic motion in the system will increase, and thereby, it will improve the ionic conductivity [13].

Additionally, it is also obvious from Figure 4 that the ionic conductivity enhances markedly with the increase in IL content, which is attributed to the increase of amorphous content by the plasticization of BMMIM-TFSI. When the IL content reaches 50%, the sample PIL-IL-0.50 presents a higher ionic conductivity, 1.07×10^{-3} S cm^{-1} at 60°C (see Table II); however, it was lower than that of the pure IL, BMMIM-TFSI (6.17×10^{-3} S cm^{-1}).[27] As the sample had higher ionic conductivity, the next electrochemical characterizations were performed with it.

Electrochemical Stability

Electrochemical stability of the polymer electrolyte was characterized by LSV on Li/PIL-IL-0.50/SS cells. In Figure 5, we can observe that the value of the onset voltage is associated with the anodic decomposition voltage. The polymer electrolyte decomposes at about 4.0 V versus Li/Li^+ (corresponding to a current density of 10 μA cm^{-2}) at 60°C. The result demonstrates that the electrolyte has good electrochemical stability, thus confirming their feasibility for application in lithium ion batteries at elevated temperature.

Lithium Redox in the Polymer Electrolyte

Lithium redox in the PIL-based electrolyte sample, PIL-IL-0.50, was characterized by cyclic voltammograms, as seen in Figure 6. The plating of lithium on the nickel electrode can be clearly observed like BMMIM-TFSI electrolyte.[22] In the first cycle for the gel polymer electrolyte, the plating of lithium is about −0.23 V versus Li/Li^+, and the anodic peak at about 0.13 V in the returning scan corresponds to the stripping of lithium, which indicate that the electrolyte can meet the requirement of the lithium ion transportation. In addition, after five cycles, the redox curve and peak values are not changed apparently, which means that the electrolyte has good cycle stability.

Table II. Ionic Conductivity of PIL-(BMMIM-TFSI)-LiTFSI-SiO_2 Electrolytes at Different Temperatures

	Ionic conductivity (S cm^{-1})					
	Temperature (°C)					
Sample name	25	30	40	50	60	70
PVE-IL-0.40	3.47×10^{-5}	5.37×10^{-5}	1.12×10^{-4}	2.39×10^{-4}	4.68×10^{-4}	8.71×10^{-4}
PVE-IL-0.45	5.01×10^{-5}	7.24×10^{-5}	1.58×10^{-4}	3.24×10^{-4}	6.76×10^{-4}	2.04×10^{-4}
PVE-IL-0.50	7.41×10^{-5}	1.07×10^{-4}	2.40×10^{-4}	5.12×10^{-4}	1.07×10^{-3}	2.04×10^{-3}

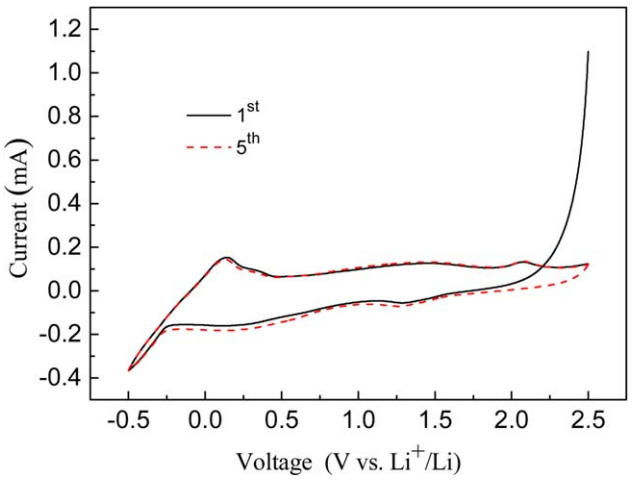

Figure 6. Cyclic voltammograms for the PVE-IL-0.50 electrolyte. Working electrode: Ni; counter electrode and reference electrode: lithium; scan rate: 10 mV s^{-1}. [Color figure can be viewed in the online issue, which is available at wileyonlinelibrary.com.]

Performances of the Batteries

$Li/LiFePO_4$ batteries with the electrolyte PIL-IL-0.5 were assembled, and their cycling performances were estimated at 60°C, as shown in Figure 7. After an initial increase, which may be a result of the generation of improved penetration and contact of the IL component from the electrolyte into the electrode material,[13,29] the cell discharged a maximum capacity of about 151 mAh g^{-1} at 0.1 C. In addition, the cell was cycled for 100 cycles with a capacity fading of ~0.05 mAh g^{-1} per cycle. After 100 cycles, the discharged capacity of the battery still retained 146 mAh g^{-1}. When compared with the tetraalkylammonium-based PIL electrolyte,[12,30] the performance of batteries with the imidazolium-based PIL electrolyte is rather better. During the overall cycling test, the coulombic efficiency, determined by the ratio between the discharge and charge capacity, is very close to 100%. In particular, the efficiency average value is more than 96%, which indicates that the cell has good cycling reversibility.

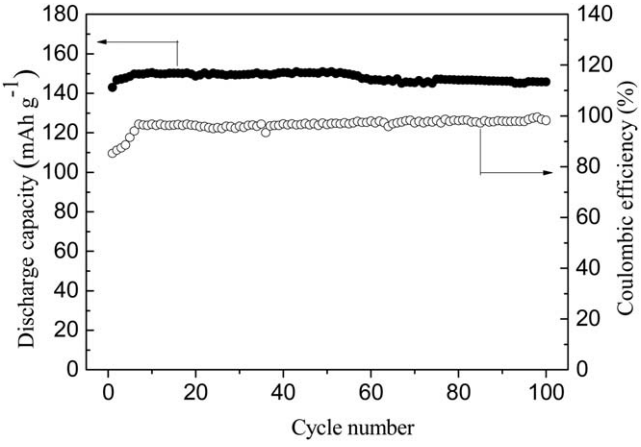

Figure 7. Discharge capacity and coulombic efficiency as functions of cycle number for $Li/PVE-IL-0.50/LiFePO_4$ cells at 60°C. Charge-discharge current rate is 0.1 C.

CONCLUSIONS

A new kind of PIL based on imidazolium cations was synthesized by homopolymerization and anion exchange reaction. The polymer electrolytes based on the PIL as polymer host and containing BMMIM-TFSI ionic liquid, LiTFSI salt, and nanosilica were prepared. With the increase of the IL, the ionic conductivity of the PIL electrolyte samples increase distinctly. The PIL electrolyte presents a higher ionic conductivity, and it is 1.07×10^{-3} S cm^{-1} at 60°C, when the IL content reaches 60% (the weight ratio of BMMIM-TFSI/PIL). Preliminary battery tests indicate that $Li/LiFePO_4$ cells with the PIL-IL-0.5 electrolytes are capable to deliver above 145 mAh g^{-1} at 60°C with very good capacity retention.

ACKNOWLEDGMENTS

This work received financial support from the Natural Science Foundation of Shaan Xi Province (Grant No. 2013JM2010), the National Natural Science Foundation of China (Grant No. 21303132), and the Postdoctoral Foundation of China (Grant No. 2012M511991).

REFERENCES

1. Xiong, Y.; Wang, H.; Wang, R.; Yan, Y.; Zheng, B.; Wang, Y. *Chem. Commun.* **2010**, *46*, 3399.
2. Bara, J. E.; Gabriel, C. J.; Hatakeyama, E. S.; Carlisle, T. K.; Lessmann, S.; Noble, R. D.; Gin, D. L. *J. Membr. Sci.* **2008**, *321*, 3.
3. Huang, J.; Tao, C.-A.; An, Q.; Zhang, W.; Wu, Y.; Li, X.; Shen, D.; Li, G. *Chem. Commun.* **2010**, *46*, 967.
4. Weber, R. L.; Ye, Y.; Schmitt, A. L.; Banik, S. M.; Elabd, Y. A.; Mahanthappa, M. K. *Macromolecules* **2011**, *44*, 5727.
5. Li, M.; Yang, L.; Fang, S.; Dong, S. *J. Membr. Sci.* **2011**, *366*, 245.
6. Wang, G.; Wang, L.; Zhuo, S.; Fang, S.; Lin, Y. *Chem. Commun.* **2011**, *47*, 2700.
7. Lee, J. H.; Lee, J. S.; Lee, J.-W.; Hong, S. M.; Koo, C. M. *Eur. Polym. J.* **2013**, *49*, 1017.
8. Chen, H.; Choi, J.-H.; Salas-de la Cruz, D.; Winey, K. I.; Elabd, Y. A. *Macromolecules* **2009**, *42*, 4809.
9. Tarascon, J. M.; Armand, M. *Nature* **2001**, *414*, 359.
10. Xu, K. *Chem. Rev.* **2004**, *104*, 4303.
11. Appetecchi, G. B.; Kim, G. T.; Montanino, M.; Carewska, M.; Marcilla, R.; Mecerreyes, D.; De Meatza, I. *J. Power Sources* **2010**, *195*, 3668.
12. Li, M.; Yang, B.; Wang, L.; Zhang, Y.; Zhang, Z.; Fang, S.; Zhang, Z. *J. Membr. Sci.* **2013**, *447*, 222.
13. Li, M.; Yang, L.; Fang, S.; Dong, S.; Hirano, S.-I.; Tachibana, K. *Polym. Int.* **2012**, *61*, 259.
14. Li, M.; Yang, L.; Fang, S.; Dong, S.; Hirano, S.-I.; Tachibana, K. *J. Power Sources* **2011**, *196*, 8662.
15. Li, M.; Dong, S.; Fang, S.; Yang, L.; Hirano, S.-I.; Hu, J.; Huang, X. *J. Appl. Electrochem.* **2012**, *42*, 851.

16. Seki, S.; Ohno, Y.; Miyashiro, H.; Kobayashi, Y.; Usami, A.; Mita, Y.; Terada, N.; Hayamizu, K.; Tsuzuki, S.; Watanabe, M. *J. Electrochem. Soc.* **2008**, *155*, A421.
17. Sato, T.; Maruo, T.; Marukane, S.; Takagi, K. *J. Power Sources* **2004**, *138*, 253.
18. Pont, A.-L.; Marcilla, R.; De Meatza, I.; Grande, H.; Mecerreyes, D. *J. Power Sources* **2009**, *188*, 558.
19. Umebayashi, Y.; Mitsugi, T.; Fukuda, S.; Fujimori, T.; Fujii, K.; Kanzaki, R.; Takeuchi, M.; Ishiguro, S. I. *J. Phys. Chem. B* **2007**, *111*, 13028.
20. Sirisopanaporn, C.; Fernicola, A.; Scrosati, B. *J. Power Sources* **2009**, *186*, 490.
21. Ye, H.; Huang, J.; Xu, J. J.; Khalfan, A.; Greenbaum, S. G. *J. Electrochem. Soc.* **2007**, *154*, A1048.
22. Raghavan, P.; Zhao, X.; Manuel, J.; Chauhan, G. S.; Ahn, J.-H.; Ryu, H.-S.; Ahn, H.-J.; Kim, K.-W.; Nah, C. *Electrochim. Acta* **2010**, *55*, 1347.
23. Ferrari, S.; Quartarone, E.; Mustarelli, P.; Magistris, A.; Fagnoni, M.; Protti, S.; Gerbaldi, C.; Spinella, A. *J. Power Sources* **2010**, *195*, 559.
24. Abraham, K. M.; Jiang, Z.; Carroll, B. *Chem. Mater.* **1997**, *9*, 1978.
25. Zhang, P.; Yang, L. C.; Li, L. L.; Ding, M. L.; Wu, Y. P.; Holze, R. *J. Membr. Sci.* **2011**, *379*, 80.
26. Hu, X. L.; Hou, G. M.; Zhang, M. Q.; Rong, M. Z.; Ruan, W. H.; Giannelis, E. P. *J. Mater. Chem.* **2012**, *22*, 18961.
27. Bonhôte, P.; Dias, A.-P.; Papageorgiou, N.; Kalyanasundaram, K.; Grätzel, M. *Inorg. Chem.* **1996**, *35*, 1168.
28. Pawlicka, A.; Danczuk, M.; Wieczorek, W.; Zygadło-Monikowska, E. *J. Phys. Chem. A* **2008**, *112*, 8888.
29. Shin, J. H.; Henderson, W. A.; Passerini, S. *J. Electrochem. Soc.* **2005**, *152*, A978.
30. Li, M.; Wang, L.; Yang, B.; Du, T.; Zhang, Y. *Electrochim. Acta* **2014**, *123*, 296.